Engineering heavily doped silicon for broadband absorber in the terahertz regime

Mingbo Pu, Min Wang, Chenggang Hu, Cheng Huang, Zeyu Zhao, Yanqin Wang, and Xiangang Luo*

State Key Laboratory of Optical Technologies for Microfabrication, Institute of Optics and Electronics, Chinese Academy of Science, P.O.Box 350, Chengdu 610209, China

lxg@ioe.ac.cn

Abstract: Highly efficient absorber is of particular importance in terahertz regime as naturally occurring materials with frequency-selective absorption in this frequency band is difficult to find. Here we present the design and characterization of a broadband terahertz absorber based on heavily Boron-doped silicon (0.7676 Ω cm) grating. It is numerically demonstrated by utilizing both the zero- and first order diffraction in the doped silicon wafer, relative absorption bandwidth larger than 100% can be achieved. Furthermore, the design can be easily extended to higher frequencies as the optical property of doped silicon is tunable through changing the doping concentration.

OCIS codes: (50.6624) Subwavelength structures; (160.3918) Metamaterials.

References and Links

1. N. I. Landy, S. Sajuyigbe, J. J. Mock, D. R. Smith, and W. J. Padilla, "Perfect metamaterial absorber," Phys. Rev. Lett. **100**(20), 207402 (2008).
2. H. Tao, C. M. Bingham, A. C. Strikwerda, D. Pilon, D. Shrekenhamer, N. I. Landy, K. Fan, X. Zhang, W. J. Padilla, and R. D. Averitt, "Highly flexible wide angle of incidence terahertz metamaterial absorber: Design, fabrication, and characterization," Phys. Rev. B **78**(24), 241103 (2008).
3. X. Liu, T. Starr, A. F. Starr, and W. J. Padilla, "Infrared spatial and frequency selective metamaterial with near-unity absorbance," Phys. Rev. Lett. **104**(20), 207403 (2010).
4. M. Diem, T. Koschny, and C. M. Soukoulis, "Wide-angle perfect absorber/thermal emitter in the terahertz regime," Phys. Rev. B **79**(3), 033101 (2009).
5. M. Pu, C. Hu, M. Wang, C. Huang, Z. Zhao, C. Wang, Q. Feng, and X. Luo, "Design principles for infrared wide-angle perfect absorber based on plasmonic structure," Opt. Express **19**(18), 17413–17420 (2011).
6. H. Tao, N. I. Landy, C. M. Bingham, X. Zhang, R. D. Averitt, and W. J. Padilla, "A metamaterial absorber for the terahertz regime: Design, fabrication and characterization," Opt. Express **16**(10), 7181–7188 (2008).
7. Q.-Y. Wen, H.-W. Zhang, Y.-S. Xie, Q.-H. Yang, and Y.-L. Liu, "Dual band terahertz metamaterial absorber: Design, fabrication, and characterization," Appl. Phys. Lett. **95**(24), 241111 (2009).
8. X. Shen, T. J. Cui, J. Zhao, H. F. Ma, W. X. Jiang, and H. Li, "Polarization-independent wide-angle triple-band metamaterial absorber," Opt. Express **19**(10), 9401–9407 (2011).
9. Y. Q. Ye, Y. Jin, and S. He, "Omnidirectional, polarization-insensitive and broadband thin absorber in the terahertz regime," J. Opt. Soc. Am. B **27**(3), 498–504 (2010).
10. J. Grant, Y. Ma, S. Saha, A. Khalid, and D. R. S. Cumming, "Polarization insensitive, broadband terahertz metamaterial absorber," Opt. Lett. **36**(17), 3476–3478 (2011).
11. C. Wu and G. Shvets, "Design of metamaterial surfaces with broadband absorbance," Opt. Lett. **37**(3), 308–310 (2012).
12. Y. Cui, K. H. Fung, J. Xu, H. Ma, Y. Jin, S. He, and N. X. Fang, "Ultrabroadband light absorption by a sawtooth anisotropic metamaterial slab," Nano Lett. **12**(3), 1443–1447 (2012).
13. D.-H. Kim, D.-S. Kim, S. Hwang, and J.-H. Jang, "Surface relief structures for a flexible broadband terahertz absorber," Opt. Express **20**(15), 16815–16822 (2012).
14. K. B. Alici, A. B. Turhan, C. M. Soukoulis, and E. Ozbay, "Optically thin composite resonant absorber at the near-infrared band: a polarization independent and spectrally broadband configuration," Opt. Express **19**(15), 14260–14267 (2011).
15. Q. Feng, M. Pu, C. Hu, and X. Luo, "Engineering the dispersion of metamaterial surface for broadband infrared absorption," Opt. Lett. **37**(11), 2133–2135 (2012).
16. K. N. Rozanov, "Ultimate thickness to bandwidth ratio of radar absorbers," IEEE Trans. Antenn. Propag. **48**(8), 1230–1234 (2000).

#175001 - $15.00 USD Received 27 Aug 2012; revised 21 Sep 2012; accepted 4 Oct 2012; published 25 Oct 2012

17. T. D. Corrigan, D. H. Park, H. D. Drew, S.-H. Guo, P. W. Kolb, W. N. Herman, and R. J. Phaneuf, "Broadband and mid-infrared absorber based on dielectric-thin metal film multilayers," Appl. Opt. **51**(8), 1109–1114 (2012).
18. A. J. Hoffman, L. Alekseyev, S. S. Howard, K. J. Franz, D. Wasserman, V. A. Podolskiy, E. E. Narimanov, D. L. Sivco, and C. Gmachl, "Negative refraction in semiconductor metamaterials," Nat. Mater. **6**(12), 946–950 (2007).
19. G. V. Naik, A. Boltasseva," Semiconductors for plasmonics and metamaterials," Phys. Status Solidi-R. **4**(10), 295–297 (2010).
20. M. Laroche, F. Marquier, R. Carminati, and J. Greffet, "Tailoring silicon radiative properties," Opt. Commun. **250**(4-6), 316–320 (2005).
21. C. H. Sun, W. L. Min, N. C. Linn, P. Jiang, and B. Jiang, "Templated fabrication of large area subwavelength antireflection gratings on silicon," Appl. Phys. Lett. **91**(23), 231105 (2007).
22. M. Wang, C. Hu, M. Pu, C. Huang, Z. Zhao, Q. Feng, and X. Luo, "Truncated spherical voids for nearly omnidirectional optical absorption," Opt. Express **19**(21), 20642–20649 (2011).
23. S. Nashima, O. Morikawa, K. Takata, and M. Hangyo, "Measurement of optical properties of highly doped silicon by terahertz time domain reflection spectroscopy," Appl. Phys. Lett. **79**(24), 3923–3925 (2001).
24. M. Pu, Q. Feng, M. Wang, C. Hu, C. Huang, X. Ma, Z. Zhao, C. Wang, and X. Luo, "Ultrathin broadband nearly perfect absorber with symmetrical coherent illumination," Opt. Express **20**(3), 2246–2254 (2012).
25. B. V. Zeghbroeck, *Principles of Semiconductor Devices* (Boulder, 1997).
26. J. Shin, J. Shen, P. B. Catrysse, and S. Fan, "Cut-through metal slit array as an anisotropic metamaterial film," IEEE J. Sel. Top. Quantum Electron. **12**(6), 1116–1122 (2006).

1. Introduction

Metamaterial (MM) perfect absorber has attracted much attention in recent years with potential applications in bolometers, solar cells and stealth technology [1–5]. This concept is of particular importance in terahertz frequencies due to the lack of easily accessible frequency-selective absorptive material [2, 4, 6, 7]. Nevertheless, most of current MM absorbers are intrinsically narrowband due to the resonant characteristics. In order to overcome the problem, dual-band [7] and triple-band [8] MM absorbers are proposed by various groups. More recently, broadband absorbers have also been investigated by utilizing the concept of multiple resonances [9–11] and gradual impedance matching [12, 13] as well as frequency dispersion engineering [14, 15].

Generally, the maximal absorption bandwidth is limited by the optical thickness as indicated by the thickness-bandwidth ratio [16]. For absorbers working at terahertz and higher frequencies, the physical thickness is very small even for quite large optical thickness. As a result, the thickness is not a big problem for broadband absorption at these frequencies. In contrary, the fabrication technique becomes a challenge since most of broadband absorbers require multilayer thin films or complicated structures [17].

In this paper, we focus on the design of broadband absorber based on doped silicon, which has been considered as a new kind of metamaterial [18, 19] and used for tailoring the radiative properties [20]. When the working frequency is larger than the plasmon frequency, doped silicon behaves as a highly lossy dielectric material. Yet, a doped silicon slab by itself is not a good absorber due to the impedance mismatch between the silicon slab and free space. The power reflection at the interface is larger than 28% for refractive index $n = 3.3$, which is similar with non-doped silicon. In order to reduce the reflection and enhance transmission (the case for non-doped silicon) or absorption (the case for doped silicon), antireflection techniques should be used. In the framework of transmission enhancement, the period of the grating structure should be in deep subwavelength scale to suppress non-zero-order diffractions [22]. However, for high efficient absorber, here we show that the absorption bandwidth can be dramatically increased by utilizing both the zero- and first order diffractions. Compared with previous broadband absorbers, the structure proposed here is mechanically stable and much easier to fabricate.

2. Principle and simulation

The binary grating considered here is characterized by the period p, groove depth t and groove width w. As illustrated in Fig. 1(a), when the period of the grating is less than the wavelength in the doped silicon, the transmission (zero-order diffraction) into the lossy substrate can be

#175001 - $15.00 USD Received 27 Aug 2012; revised 21 Sep 2012; accepted 4 Oct 2012; published 25 Oct 2012

totally absorbed if there is no reflection. As the frequency increases, the first order diffraction in the silicon substrate takes place (Fig. 1(b)) while there is still only zero-order backward diffraction because the refractive index of doped silicon is much larger than that of free space. Thus, there are two absorption mechanisms in the grating for different working frequencies. In general, the first absorption mechanism can be well described by effective medium theory (EMT) [22], where the subwavelength structure is treated as an equivalent medium with quarter-wavelength thickness. To utilize the first order diffraction, however, the period of the structure should be larger than the wavelength in the silicon but still smaller than that in free space ($\lambda / n < p < \lambda$). By properly choosing the period and other geometrical parameters, it is possible to combine the two absorption peaks and enhance the absorption bandwidth.

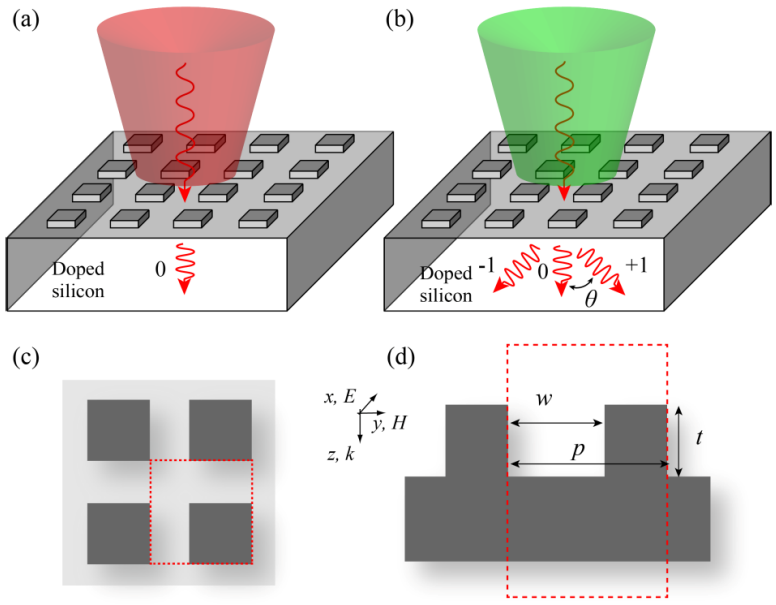

Fig. 1. Schematic of diffraction when illuminated at two different frequencies. (a) Only zero-order diffraction occurs in the substrate at low frequency. (b) First order diffraction in the substrate occurs at higher frequency. (c) and (d) are the front and side views of the structure. The rectangular region in (c) and (d) is the unit cell used in simulations.

Based on the above considerations, a 500 μm thick Boron-doped silicon wafer is chosen here. The sample can be easily fabricated and measured by terahertz time domain spectroscopy (THz-TDS) [23]. In the numerical simulations, finite element method (FEM) method is used to calculate the absorption efficiency with periodic boundary condition in x and y directions. As the doped silicon is very lossy and thick enough, the transmission is zero and the absorption can be calculated as $A = 1\text{-}R$, where $R = r^2$ is the reflectance spectrum. The complex dielectric constant ($\varepsilon = n^2$, where n is the refractive index) of the doped silicon is described by Drude model [24]:

$$\varepsilon = \varepsilon_\infty - \frac{\omega_p^2}{\omega(\omega + i\Gamma)}, \tag{1}$$

where $\varepsilon_\infty = 11.7$ is the dielectric constant of non-doped silicon. $\Gamma = 1/\tau$ is the carrier scattering rate, and ω_p is the plasma frequency defined by $\omega_p^2 = N_c e^2 / (\varepsilon_0 m^*)$. Here N_c is the carrier density, e is the electronic charge, ε_0 is the permittivity of vacuum, and m^* is the effective carrier mass taken as $0.26m_0$, where m_0 is the free electron mass. Since N_c is chosen as 2e16

#175001 - $15.00 USD Received 27 Aug 2012; revised 21 Sep 2012; accepted 4 Oct 2012; published 25 Oct 2012

cm^{-3} in this paper, the corresponding plasma frequency and scattering rate can be calculated using experimental results [25] as ω_p = 15.6 THz and Γ = 16.5 THz with static resistivity of ρ = 0.77 Ω cm.

Firstly, the absorption around 2 THz is optimized for largest operation bandwidth (Sample1). The optimized geometrical parameters are p = 63 μm, w = 25 μm, and t = 30 μm. As shown in Fig. 2, there are two absorption peaks at 1.5 THz and 2.3 THz, arising from the zero- and first order diffraction, respectively. The −10 dB (A>0.9) absorption bandwidth is larger than 2 THz and the corresponding relative bandwidth is larger than 100%. To illustrate the influence of the period of grating, another absorber with absorption peak at 1.5 THz with smaller period is designed with p = 30 μm, w = 8 μm, and t = 26 μm (Sample2). In this case, the first order diffraction induced absorption peak shift to higher frequency (3.2 THz) and the absorption is only 0.85. In addition, the case when grating is replaced by an equivalent layer with quarter-wavelength thickness is also shown. Clearly, the equivalent layer is not a good choice since its absorption bandwidth is only half of that for Sample1. As a result, the proper selection of the period is a key point in the design of this kind of broadband absorber.

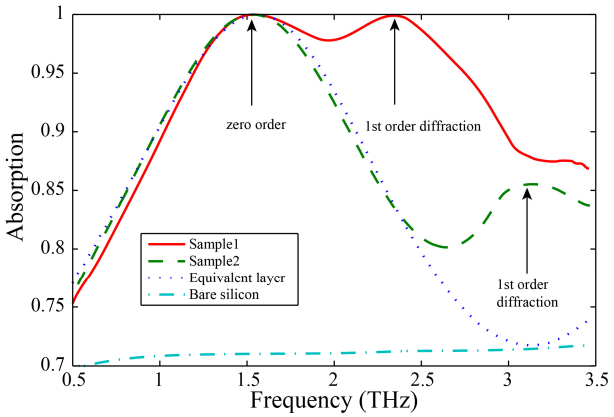

Fig. 2. Absorption spectra of samples with different periods. The cases for a bare doped silicon slab and an absorber based on quarter-wavelength antireflection layer are also shown.

To further comprehend the physical origin of the two absorption peaks, the diffraction is investigated using rigorous coupled wave analysis (RCWA). For simplicity a one-dimensional absorber with p = 63 μm, w = 27 μm, and t = 31 μm is used in the simulation. As shown in Fig. 3(a), the absorption curve for transverse magnetic (TM) polarization (magnetic field is along y direction) is similar with the two-dimensional grating (Sample1), while the two absorption peaks shift to 1.4 THz and 2.25 THz.

The diffraction efficiencies (DE) for different periods are illustrated in Fig. 3(b). Obviously, the first absorption peak (around 1.4 THz) keeps almost unchanged while the second absorption peak shifts to lower frequencies when the period increases. At proper period, the two absorption peaks are connected to form a large absorption bandwidth. As illustrated in Fig. 3(c) and (d), the minimum of the reflectance R and zeroth order transmittance T_0 are in coincidence with the maximum of first order diffraction. This fact further proves that the second absorption peak is determined by the first order diffraction. In general, the first order diffraction angle can be described by the grating equation:

$$\sin\theta = \lambda / (np). \tag{2}$$

The calculated first order diffraction angle at 2.25 THz for p = 63 μm is about 40°. Obviously, the working frequency is inversely proportional to the period.

#175001 - $15.00 USD Received 27 Aug 2012; revised 21 Sep 2012; accepted 4 Oct 2012; published 25 Oct 2012

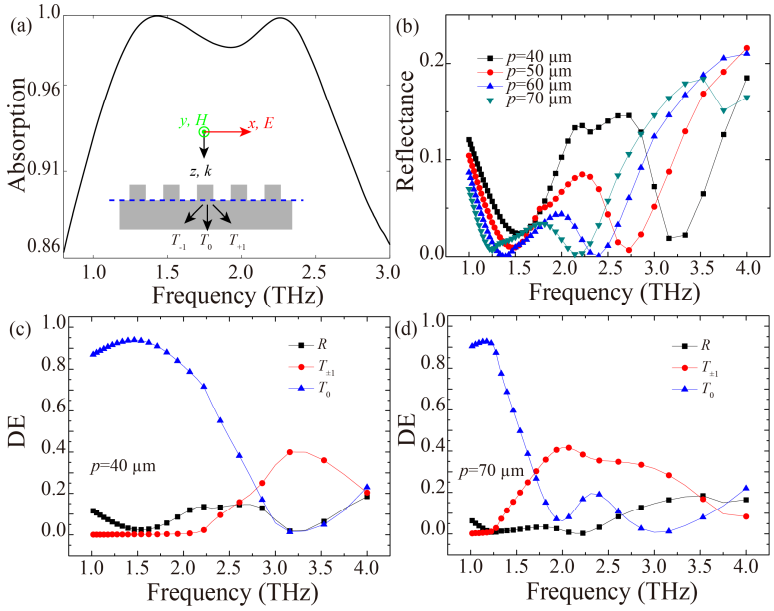

Fig. 3. (a) Absorption of the 2D grating structure. (b) Reflectance for different periods with the same thickness and filling ratio. (c) (d) Diffraction efficiency of the different order diffraction for p = 40 μm and 70 μm.

As indicated in above discussion, the first absorption peak at 1.4 THz can be interpreted by effective medium theory. In the limit of deep subwavelength period, the effective permittivity can be written as [22]:

$$\varepsilon_{eff} = \frac{(1+\eta)\varepsilon_{si}}{1+\eta\varepsilon_{si}}, \tag{3}$$

where $\eta = w/(p-w)$. However, this expression is not valid any more when the period is not in deep subwavelength scale. As shown in Fig. 4(a), the grating structure can be viewed as a waveguide array at higher frequencies such as 2.25 THz. The electromagnetic fields are concentrated in the air region which can be treated as a waveguide with an effective impedance of about $Z_{eff} = (w/p)Z_0 = 0.43Z_0$ and refractive index near 1 [26]. Meanwhile, the impedance of 1st order diffraction at 2.25 THz is $Z_s = Z_0 \cos\theta / n = 0.22Z_0$. Since the zero order transmission T_0 is zero at 2.25 THz, the antireflection condition, defined as $Z_{eff} = \sqrt{Z_0 Z_s} = 0.47Z_0$ can be fulfilled. Also, the working frequency is very close to that determined by $c/(4t) = 2.5$ THz, where c is light speed in vacuum.

#175001 - $15.00 USD Received 27 Aug 2012; revised 21 Sep 2012; accepted 4 Oct 2012; published 25 Oct 2012

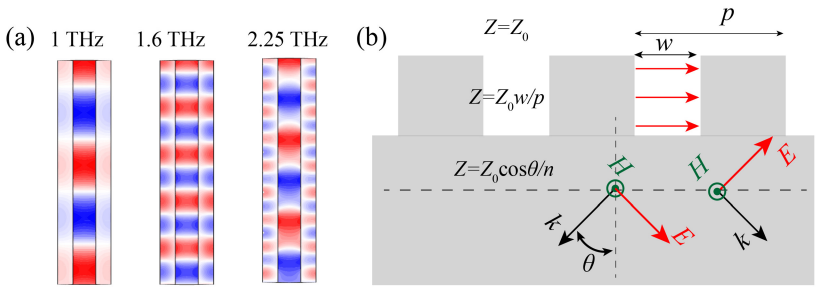

Fig. 4. (a) Horizontal Electric fields distributions at different frequencies for an infinite thick grating. (b) Schematic of the impedance matching for 1st order diffraction.

It is also interesting to investigate whether second order or higher order diffraction can be utilized to increase the absorption bandwidth. As shown in Fig. 5, the diffraction at higher frequencies is calculated for a two layer grating. The period is keeps as p = 63 μm while w_1, w_2, t_1, and t_2 are optimized as 12.5 μm, 38 μm, 20 μm and 20 μm. Obviously, the three absorption peaks located at 1.2 THz, 2.2 THz and 3.7 THz are in coincidence with the peaks of T_0, $T_{\pm 1}$, $T_{\pm 2}$. The absorption is larger than 90% for frequencies between 1 to 4 THz. Further increase of layers may lead to larger bandwidth. Nevertheless, the fabrication process will become more complex and the thickness will become larger.

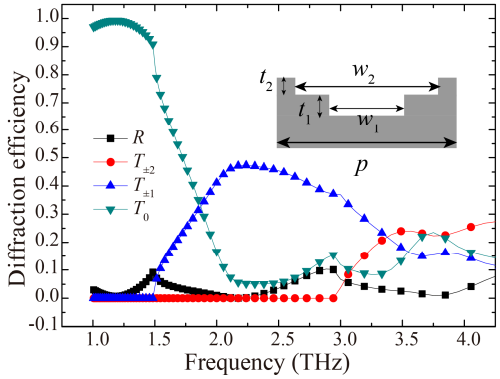

Fig. 5. Diffraction efficiencies of a two layer doped silicon grating as shown in the inset.

In order to investigate performance of the absorber (Sample1) at oblique incidences, the absorption at different incidence angles for different polarizations are calculated and illustrated in Fig. 6. Obviously, although the absorption deteriorate for angles larger than 40°, the absorption below this angle is very good, especially for TE polarizations.

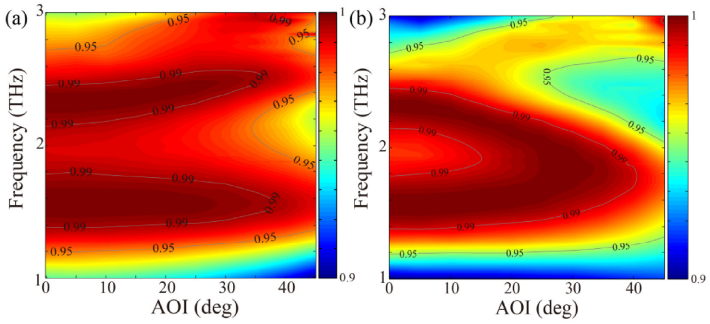

Fig. 6. Dependences of the absorption with angle of incidences for (a) TE polarization and (b) TM polarization.

#175001 - $15.00 USD Received 27 Aug 2012; revised 21 Sep 2012; accepted 4 Oct 2012; published 25 Oct 2012

Finally, it is expected that the absorption property can be scaled to other frequency bands by scaling the geometrical parameters due to the scaling principle of Maxwell's equations [4]. However, this is not a trivial problem for traditional absorber as material loss for normal material is frequency dependent at terahertz and optical frequencies. For the doped silicon used here, the dielectric constant and loss can be tuned by doping concentration. Thus, the broadband absorber can be easily extended to higher frequencies by scaling the doping concentration and geometrical parameters simultaneously. In order to demonstrate the scaling possibility, the geometrical parameters of Sample1 are reduced by 15 times and the doping concentrating is increased by 500 times (N_c = 1e19 cm^{-3} and ρ = 0.0088 Ω cm). After some iterations of optimization, the geometrical parameters are chosen as p = 4 μm, w = 1.5 μm, and t = 1.8 μm. Meanwhile, the total thickness needed is only 20 μm, which is much smaller than the thickness of the wafer. As shown in Fig. 7, the absorption spectrum is similar with that of Sample1 and the relative absorption bandwidth for A>0.9 is also larger than 100%.

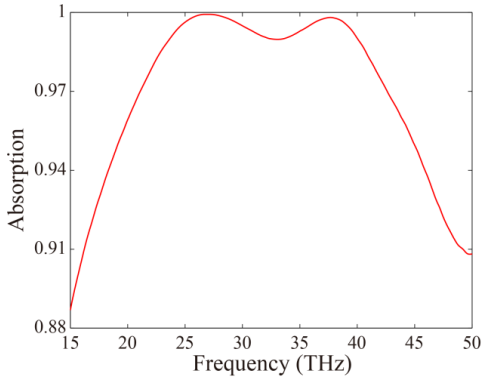

Fig. 7. Absorption of the scaled absorber for mid-infrared frequencies.

3. Conclusion

In summary, this paper presents the design and characterization of a high efficient terahertz absorber based on a binary grating on heavily doped silicon. The period of the grating is properly chosen to make the two absorption peaks due to zero- and first diffraction become near in frequency to enhance the working bandwidth. Furthermore, it has been demonstrated the use of doped silicon is of particular importance for the scaling of design in frequencies. Thus, the structured doped silicon provides a general solution for broadband absorption in spectra ranging from several terahertzes to near infrared frequencies. For frequencies less than 1 THz, however, the performance is restricted by the overall thickness of silicon wafer (typically 500μm). Finally, it is also interesting to note that the concentration or mobility of the carriers in doped semiconductor could be changed therefore lead to a tunable structure with a proper optical or THz excitation. Therefore the different order diffractions as well as the absorption bandwidth may be tunable.

Acknowledgment

This work was supported by 973 Program of China (No. 2011CB301800) and National Natural Science Funds for Distinguished Young Scholar (No. 60825405).

#175001 - $15.00 USD Received 27 Aug 2012; revised 21 Sep 2012; accepted 4 Oct 2012; published 25 Oct 2012